Systematic Control of the Electrical Conductivity of Poly(3,4-ethylenedioxythiophene) via Oxidative Chemical Vapor Deposition

Sung Gap Im and Karen K. Gleason*

Department of Chemical Engineering and Institute for Soldier Nanotechnologies, Massachusetts Institute of Technology, Cambridge, Massachusetts 02139

Received December 12, 2006; Revised Manuscript Received June 24, 2007

ABSTRACT: Systematic variation in the electrical conductivity of poly(3,4-ethylenedioxythiophene) (PEDOT) was achieved by oxidative chemical vapor deposition (oCVD). For oCVD, both the oxidant, Fe(III)Cl_3, and 3,4-ethylenedioxythiophene (EDOT) monomer are introduced in the vapor phase. A heated crucible allows for sublimation of the oxidant directly into the reactor chamber operating at 150 mTorr. Spontaneous reaction of the oxidant with the monomer introduced though a feedback-controlled mass flow system results in the rapid (>200 nm thick film in 30 min) formation of π-conjugated PEDOT thin films directly onto a temperature-controlled substrate. As the substrate temperature is increased from 15 to 110 °C, increasing conjugation length, doping level, and electrical conductivity of the PEDOT chains are observed by UV−vis absorption spectroscopy (UV−vis), Fourier transform infrared spectroscopy (FTIR), and Raman spectroscopy. Concomitantly, the measured electrical conductivity of the PEDOT films increases systematically with an apparent activation energy of 28.2 ± 1.1 kcal/mol.

Introduction

Conjugated polymers offer the advantages of high flexibility as compared to conventional electrically conductive inorganic materials.[1,2] One of the most promising conducting polymers is poly(3,4-ethylenedioxythiophene) (PEDOT),[1−3] in which the 3- and 4-positions of the thiophene ring are blocked by oxygen, minimizing unwanted polymerization at these two β-carbon sites. Moreover, the oxygen acts as an electron-donating group, increasing the electron density of the thiophene ring. Therefore, the conjugated polythiophene ring can easily be positively charged by the anion dopants. The opposite side of oxygen atoms is capped by an ethylene moiety to form a stable six-membered ring. This back-bonded ring minimizes the unwanted polymerization reaction branched from the 3- and/or 4-position.

The methods for forming thin films comprised solely of a conductive polymer, such as PEDOT, are limited by the rigid nature of the conjugated backbone.[4] Neither spin-casting from solution nor melt-processing can be used. High-conductivity (∼300 S/cm) PEDOT thin films have been synthesized by electropolymerization,[5,6] but a conductive substrate is required. Oxidative polymerization can also yield PEDOT thin film,[7,8] but it is not trivial to reproducibly obtain highly conductive films.[9]

An alternate approach to create PEDOT films is the use of "flexible polymer dopants" to make the solution process of conjugated polymers possible. One of the most successful combinations is PEDOT doped with poly(styrenesulfonic acid) (PSS) water emulsion developed by scientists at Bayer AG (commercial name of Baytron P).[3,10,11] Even though the conjugated PEDOT film can be made with this emulsion, the conductivity is inherently low (less than 10 S/cm). In addition, a complicated additional hydrophilic substrate treatment such as oxygen plasma treatment or UV-ozone treatment must be applied to achieve a uniform polymer film.[12]

* To whom correspondence should be addressed: e-mail kkg@mit.edu; phone (617) 253-5066; Fax (617) 258-5042.

Chemical vapor deposition (CVD) of PEDOT films has several potential benefits. Substrates which are not electrically conductive or which can be degraded by solvent can also be used, including paper, fabric, glass, wafer, and metal oxide.[13] Using the same feed gases, the CVD process conditions, such as temperature, pressure, and flow rates, can be varied to adjust the properties required for successful integration of the film into an organic devices such as organic light-emitting diodes (OLED) and organic thin film transistors (OTFT).

Recently, Winther-Jensen reported PEDOT thin film deposition in which the EDOT monomer was introduced in the vapor phase, resulting in reported conductivities as high as 1000 S/cm.[14] This method used spin-coating of the oxidizing agent of iron toluenesulfonate. Meng also introduced a CVD process using chlorinated EDOT for PEDOT.[15] Building on the idea of introducing the EDOT from the vapor phase, Lock developed an oxidative chemical vapor deposition (oCVD) method which employs the sublimation of the oxidizing agent of iron(III) chloride, obtaining a maximum conductivity of 105 S/cm.[13]

Various schemes are suggested to control the conductivity of PEDOT:PSS. By diluting the conducting polymer with nonconductive host polymer such as poly(methyl methacrylate) or poly(vinylpyrolidone), the conductivity of PEDOT:PSS was increased by a factor of 10.[1,16] By adding ethylene glycol (EG) or *meso*-erythritol into PEDOT:PSS film, the conductivity was increased from 0.4 to 200 S/cm.[17−19] By changing chemical species of dopants in electrochemically prepared PEDOT film, Groenendaal et al. could obtain various range of conductivities from 50 to 650 S/cm.[6,20] By adding base materials such as imidazole or pyridine in the course of liquid-phase or vapor-phase oxidative polymerization,[8,9,14] an enormous conductivity increase—up to more than 1000 S/cm[14]—was obtained. The most successful way of systematically controlling the conductivity to date is doping level control by electrochemistry.[6,20−22] Johansson et al. observed the conductivity variation from 6×10^{-5} to 16 S/cm by the electrochemical doping−dedoping process, but because of the extremely unstable nature of dedoped

10.1021/ma0628477 CCC: $37.00
Published on Web 08/03/2007

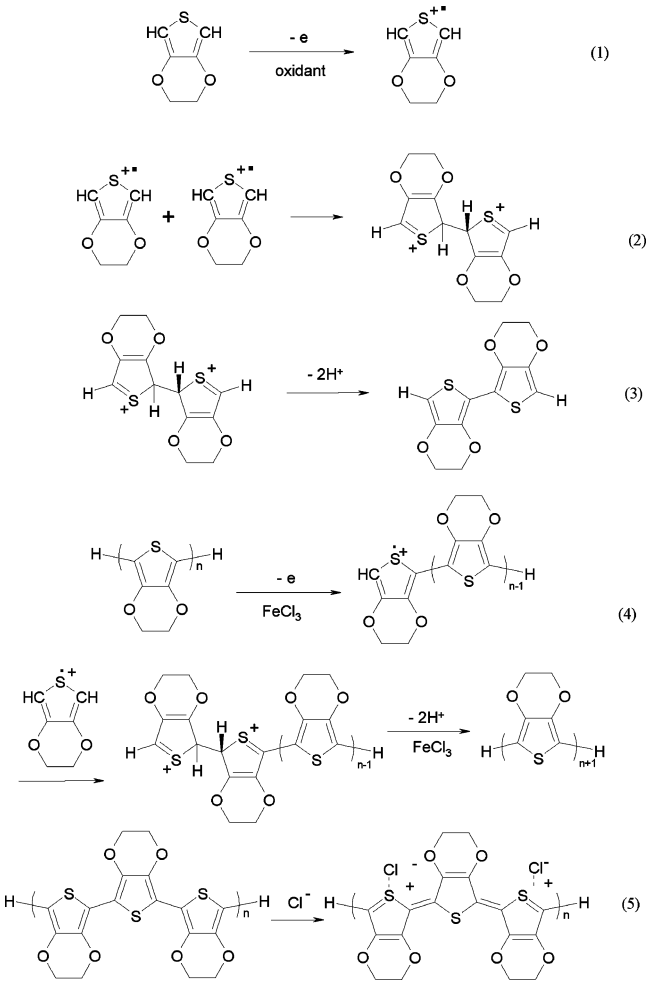

Figure 1. Proposed polymerization mechanism for oxidative polymerization of PEDOT: (1) oxidation of EDOT to from cation radical; (2) dimerization of cation radical; (3) deprotonation to form conjugation; (4) further polymerization from *n*-mer to (*n* + 1)-mer; (5) doping process of PEDOT.

PEDOT film, the low conductivity of 6×10^{-5} S/cm cannot be maintained in ambient conditions and a spontaneous doping process occurred.[22] The first report of PEDOT films prepared by the oCVD process displayed an amazingly wide span of conductivities.[13,23]

It is important to consider that the oCVD method may have many similarities to the stepwise reaction mechanism that is widely accepted for PEDOT oxidative polymerization,[2,8,13,24] which is schematically shown in Figure 1. Stoichiometric amounts of oxidizing agent react with the EDOT monomer to generate cation radicals (Figure 1, eq 1). Pairs of cation radials dimerize (Figure 1, eq 2), and the anions of oxidizing agent scavenge two protons to stabilize the dimer (Figure 1, eq 3). The oxidizing agent then acts on the dimer and again (Figure 1, eq 4). These stepwise reactions are repeated continuously to form the PEDOT polymer. Some of the positively charged thiophene rings are stabilized by the counterion in the polymer, which is referred as a dopant (Figure 1, eq 5). The doping process results in charges along the conjugated backbone of the conducting polymer which enable the flow of current. Therefore, the amount of dopant is directly related to the conductivity of conjugated polymer.[6,22] As shown in Figure 2, the type of conjugation may be distorted in the course of the doping process. The two possible types of conjugation are shown in **B** and **Q** in Figure 2.[18,25] Form **B** is often referred to as benzoid and form **Q** as quinoid. The transition energy between

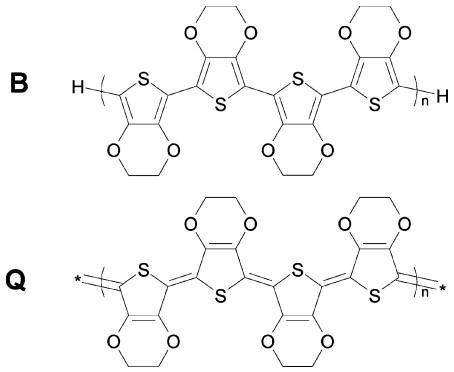

Figure 2. Benzoid (B) and quinoid (Q) types of PEDOT.

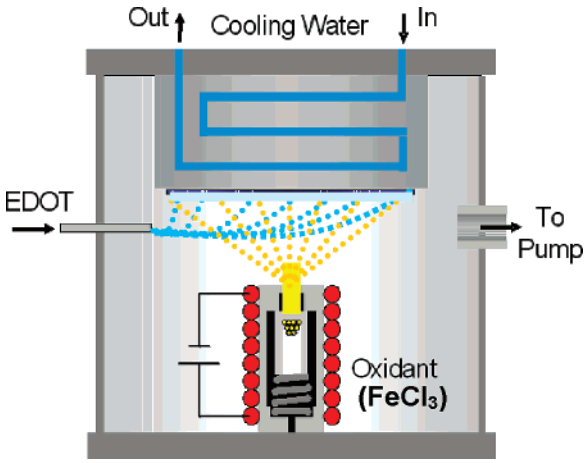

Figure 3. Schematic figure of modified oCVD process chamber.

two types is called the distortion energy which is a function of conjugation length.[26−28]

In this work, the oCVD process was tuned for maximum conductivity and reproducibility. The oCVD process provides systematic control over the final electrical conductivity of the films. Rigorous characterization methods were exploited including four-point probe measurements, profilometer, UV−vis absorption spectroscopy, Fourier transform infrared spectroscopy (FTIR), and Raman spectroscopy.

Experiments and Characterization

Previously, highly conductive PEDOT films (up to 105 S/cm) were obtained via oCVD, and this conductivity could be modulated by controlling substrate temperature and by introducing basic pyridine vapor.[13] In the current work, two important hardware changes were made in order to improve the uniformity of oxidant delivery: the chamber was inverted so that the substrate faces down to oxidant source, and the distance between the oxidant crucible and the substrate was increased to 20 cm to minimize the heating effect from the oxidant cell to the substrates. The schematic figure of newly modified oCVD process chamber is shown in Figure 3. The process conditions of the current work are similar to the previous work, but some adjustments have been made to optimize deposition for the new hardware configuration For example, the current work uses a pressure of 150 mTorr instead of the previous value of 300 mTorr. Glass slides and silicon wafers were used for substrates. The substrate temperature was controlled with cooling water and PID controlled substrate heater. The chamber pressure was controlled by a butterfly valve and was maintained at about 150 mTorr. Additional argon (grade 5.0, BOC Gases) was introduced into the crucible to maintain the process pressure of oCVD. Fe(III)Cl_3 (97%, Aldrich) was used as the oxidant without further purification. The oxidant is loaded in a porous crucible placed above the stage. The crucible was heated to a temperature

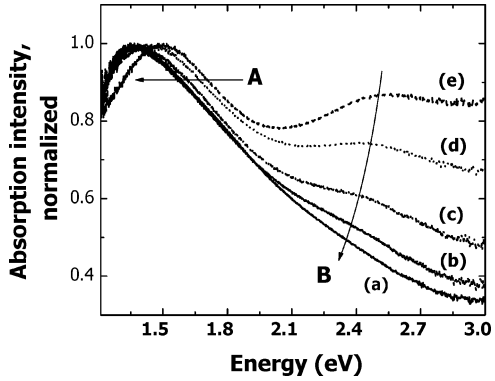

Figure 4. UV−vis optical spectra of CVD polymerized PEDOT with various substrate temperature (T_{sub}): (a) T_{sub} = 100 °C, (b) T_{sub} = 85 °C, (c) T_{sub} = 71 °C, (d) T_{sub} = 47 °C, and (e) T_{sub} = 15 °C. **A** represents the bathochromic shift of polaronic energy state with the increase of substrate temperature. **B** represents the bathochromic peak shift and intensity decrease of the π-to-π^* transition energy state with the increase of substrate temperature.

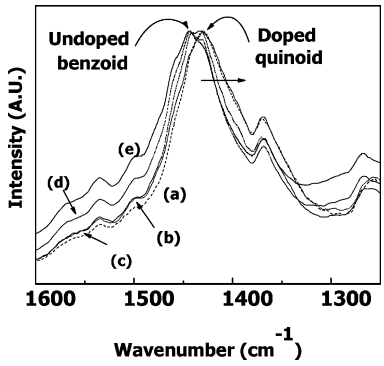

Figure 5. Overlapped Raman spectra of CVD polymerized PEDOT with various substrate temperature (T_{sub}): (a) T_{sub} = 100 °C, (b) T_{sub} = 85 °C, (c) T_{sub} = 71 °C, (d) T_{sub} = 47 °C, and (e) T_{sub} = 15 °C. Peak shift indicated by the arrow represents that the C═C conjugation is shifted from undoped benzoidal type (1444 cm^{-1}) to doped quinoidal type (1428 cm^{-1}).

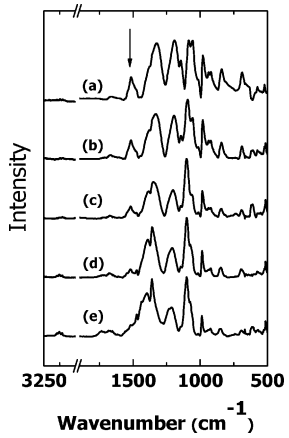

Figure 6. FT-IR spectra of PEDOT with various substrate temperature (T_{sub}): (a) T_{sub} = 100 °C, (b) T_{sub} = 85 °C, (c) T_{sub} = 71 °C, (d) T_{sub} = 47 °C, and (e) T_{sub} = 15 °C. Arrow represents the C═C stretch peak at 1520 cm^{-1}.

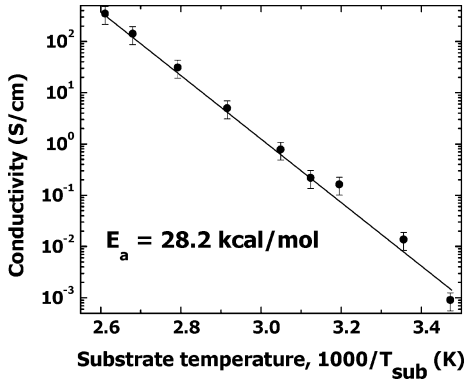

Figure 7. Arrhenius plot of substrate temperature vs conductivity.

of about 320 °C where sublimation of the oxidant set on. At the same time, vapor-phase EDOT monomer (3,4-ethylenedioxythiophene, Aldrich) was delivered into the reactor. The EDOT flow rate was set at 3 sccm. The process time was 30 min for all of the films. All the chemicals used in the experiments are used without any further purification. Substrate temperature was varied from 15 to 110 °C with other process parameters fixed. After the CVD process, the films are dried for at least 2 h in a vacuum oven heated to 70 °C at a gauge pressure of −15 in.Hg. After drying, deposited films were rinsed in methanol (HPLC Grade, J.T. Baker). The rinse step is intended to remove any unreacted monomer or oxidant in the films as well as short oligomers and reacted oxidant in the form of Fe(II)Cl_2.

The thicknesses of the films deposited on glass are measured on a Tencor P-10 profilometer. Conductivity measurements are done with a four-point probe (model MWP-6, Jandel Engineering, Ltd.) with a Keithley 236 Source-Measure Unit. A constant source current of 0.001−1 mA is applied, and the voltage is monitored. Sheet resistivity is calibrated by ITO-coated glass and copper-coated wafer. All the conductivity values are calculated using the sheet resistivity measured by the four-point probe and thickness measured by a profilometer. Films on silicon substrates were measured with FTIR (Nexus 870, Thermo Electron Corp.) and Raman spectroscopy (Kaiser Hololab, 5000R, spectra obtained with an excitation wavelength of 785 nm) for information on chemical composition. UV−vis absorption spectroscopy (Cary 5E) was also performed to monitor the energy levels of the conjugated polymer film. As the resultant PEDOT films have different film thickness, every UV−vis spectrum was normalized with respect to the peaks at 1.3−1.5 eV.

Results and Discussion

UV−Vis Absorption Spectroscopy Figure 4 represents the UV−vis absorption spectra of the oCVD PEDOT films deposited at the substrate temperature from 15 to 100 °C. In undoped PEDOT films of sufficient conjugation length, the π-to-π^* transition is observed in the range of 580−600 nm (2.0−2.2 eV).[18,21,25] In oligomeric PEDOT, the π-to-π^* transition occurs at higher energy and shifts to lower energy as the conjugation length increases.[29−31] In the series of oCVD deposited PEDOT film, the π-to-π^* transition has a maximum energy of 2.5 eV (sample e in Figure 4), and this energy decreases as the substrate temperature increases. This observation strongly infers that the conjugation length of oCVD deposited PEDOT increases systemically as the substrate temperature increases.

The doping level change of oCVD deposited PEDOT was also observed. Dopants introduce polaron and bipolaron states having energy gaps at ∼1.4 and ∼1.1 eV, respectively, for PEDOT.[21] As the doping level increases, the π-to-π^* transition energy state shifts to the lower polaronic energy state.[21] As a result, the relative intensity of the π-to-π^* transition peak decreases as the doping level increases. In Figure 4, the relative intensity of the π-to-π^* transition peak (around 2.1−2.5 eV) decreases with increasing electrical conductivity of PEDOT. The absorption spectrum of PEDOT deposited at the highest substrate temperature (sample a in Figure 4) displays that the π-to-π^* transition peak is completely overlapped by the polaronic peak, whose spectrum is very similar to that of fully doped PEDOT

Table 1. Summary of Selected Properties of oCVD Deposited PEDOT Film

substrate temperature, °C	15	47	71	85	100
conductivity, S/cm	9.1×10^{-4}	0.080	0.66	31	348
thickness, nm	85	87	72	59	63
position of C═C symmetric peak local maxima in Raman spectroscopy, cm^{-1}	1444.1	1431.3, 1442.7	1431.9, 1440.6	1430.9	1429.7
polaronic energy peak maximum in UV−vis spectroscopy, eV	1.50	1.44	1.38	1.36	1.35

film in the literature.[6] The observed absorption spectrum indicates that the doping level of PEDOT can be tuned by changing the substrate temperature in the oCVD process. A similar trend was observed in the peaks of the polaronic energy state. With increasing doping levels, the polaronic gap shifts to lower energy.[17,18,21] Thus, the observed shift of the polaronic energy peak maximum in Figure 4 from 1.5 to 1.35 eV corresponds to increased doping levels for the series of films with increasing conductivity.

The observed shifts to lower energy of both the π-to-π^* transition peak and polaronic peak and the relative reduction of π-to-π^* transition peak demonstrate that higher doping levels are achievable in oCVD PEDOT films deposited at high substrate temperature. Several previous reports have shown that longer conjugation length facilitates doping by lowering the distortion energy required.[26,27,32] Thus, increasing conjugation length with increasing deposition temperature is a straightforward hypothesis which accounts for all the trends in the UV−vis absorption data (Figure 4) which will be tested by additional characterization methods reported in the following sections.

Raman Spectroscopy. Raman spectra of the series of oCVD PEDOT films were collected (Figure 5). The obtained Raman spectra are similar to one another and have the same primary features as that of electrochemically grown PEDOT.[17,18,25,33] Characteristic peaks of well-defined PEDOT, such as symmetric C_α═C_β symmetric stretching peak at 1444 and 1428 cm^{-1} [17,18,33] and C_β═C_β stretching peak at 1368 cm^{-1} are clearly observed.[25,33]

Variation in the doping level was observed in the Raman spectrum. In PEDOT deposited at the lowest substrate temperature (sample e in Figure 5), the peak at 1444 cm^{-1} is dominant and a small shoulder of 1428 cm^{-1} peak is observed. For samples deposited at higher substrate temperature, the symmetric C_α═C_β symmetric stretching peak maximum shifts gradually from 1444 to 1428 cm^{-1}. In PEDOT deposited at the highest substrate temperature (sample a in Figure 5), the peak at 1428 cm^{-1} is dominant and a trace shoulder of 1444 cm^{-1} was observed. Ouyang et al. assigned these peaks as undoped benzoidal vibration for the peak at 1444 cm^{-1} and doped quinoidal vibration for 1428 cm^{-1} in the PEDOT:PSS film.[17,18] They also observed that the conductivity of PEDOT:PSS film was increased as the Raman peak was shifted from benzoid to quinoid.[17,18] Thus, the shift from 1444 to 1428 cm^{-1} indicates that the nature of conjugation shifts from undoped benzoid to doped quinoid and is completely consistent with the UV−vis results (Figure 4).

Fourier Transform Infrared (FTIR) Spectroscopy. Figure 6 displays the FTIR spectra of the oCVD PEDOT films produced by variation in substrate temperature from 15 to 100 °C. Even though a quantitative analysis of the FTIR spectra proved intractable due to the broadness and position shifts of the peaks from the conducting polymer films,[32] systematic changes are observed. As the substrate temperature decreases, the peak intensity of C═C stretch at 1520 cm^{-1} [33−35] gradually decreases. In the spectrum for PEDOT deposited at the lowest substrate temperature (sample e in Figure 6), a considerable part of C═C stretch at 1520 cm^{-1} is difficult to resolve. Similar spectral features are observed in undoped oligomeric PEDOT.[33,34] Therefore, the decrease in C═C stretch at 1520 cm^{-1} is a direct indication of short conjugation length. Thus, the FTIR results also support the hypothesis of higher substrate temperatures producing oCVD PEDOT films of longer conjugation length, as discussed in the previous UV−vis and Raman sections.

Conductivity. Figure 7 demonstrates that oCVD is an excellent synthesis method for achieving systematic control of electrical conductivity over a wide range of values. The measured conductivity values of oCVD PEDOT polymer films grow dramatically as the substrate temperature increases 15−110 °C, the only processing parameter which was varied. The range of conductivity achieved was from a low of 9.1×10^{-4} S/cm to a high of 348 S/cm. Thus, by a simply varying substrate temperature, the conductivity of oCVD PEDOT can be systematically controlled over a range spanning more than 5 orders of magnitude.

The Arrhenius plot of conductivity with the substrate temperature (Figure 7) fits well to a single apparent activation energy of 28.1 ± 1.1 kcal/mol. This linear relationship (R^2 > 99%) suggests that a fundamental link exists between electrical conductivity and a single thermally activated chemical reaction or diffusion step occurring at the substrate during oCVD growth.[36] Table 1 summarizes the oCVD prepared and gives selected properties.

The observed conductivity data are completely consistent with the optical and chemical analysis performed above in that oCVD PEDOT with longer conjugation length and higher doping level has a higher electrical conductivity. However, the extreme complexity of electrical conductivity of conducting polymer[37,38] makes the true nature of conductivity unclear since the electrical conductivity is a collective function of not just the conjugation length and doping level but also crystallinity,[38] interface with the substrate,[39,40] and the measurement conditions, such as frequency and temperature.[37] Nevertheless, the Arrhenius plot indicates that the conductivity has a close relationship with the substrate temperature of the oCVD process. Thus, we can reasonably postulate that the conductivity is intrinsically related with the polymerization reaction steps occurring at the surface of the substrate. At 25 °C, the EDOT monomer has limited volatility, with a vapor pressure of 0.278 Torr. Even lower vapor pressures at 25 °C are associated with the dimers (1.57×10^{-7} Torr) and trimers (1.3×10^{-13} Torr).[36] Higher order oligomers are anticipated to be essentially involatile at 25 °C and higher substrate temperature. Therefore, the oxidative polymerization reaction is confined at the surface of the substrate.

Higher temperature for surface polymerization will increase cation radical reactivity and accelerate dimerization and polymerization reactions (Figure 1, eqs 1−3) because the reaction rate constants will increase with higher temperature.[36] Thus, as reaction rates increase, monomer and oligomer cation radicals are more easily formed and then combine with each other to form stable high molecular weight chains until the high chain lengths lack the mobility limiting the mass transfer of radical cations. Chain mobility will also improve with increasing substrate temperature. In the same way, higher temperature can

also promote deprotonation reaction to form conjugation due to increased reaction rate constant at higher temperature.[36] Therefore, the extent of the deprotonation reaction is directly related to the length of conjugation.[8,13,14] Then it follows that the conjugation length is governed by molecular weight of polymer and the degree of deprotonation of the polymer chain. Moreover, the scavenged protons are easily evaporated in the form of HCl.[41] Since the back-bonded dioxyethylene ring can be possibly destroyed by acid-catalyzed reactions,[13,14,24] the rapid elimination of HCl is desirable to prevent formation of defects along the chain. Thus, high surface temperature promotes the formation of higher molecular weight chains and also decreases the density of defects along the chain caused by insufficient deprotonation or unwanted acid-catalyzed side reactions. Therefore, the conjugation length will depend upon the completeness of each stepwise polymerization reaction.

Conclusion and Outlook

The substrate temperature of the oCVD process is a critical parameter which permits control over the conductivity of PEDOT films over a range of more than 5 orders of magnitude. From FTIR and Raman spectroscopy, the chemical nature giving rise to the systematic variation in the level conduction of the PEDOT film was elucidated. Specifically, the substrate temperature controls the conjugation length of the oCVD PEDOT. Additionally, the optical absorption spectra demonstrate that the combination of lack of doping and short conjugation length lead to low values of conductivity in films deposited at low substrate temperature. From the oCVD polymerization process, a single apparent activation energy of 28.1 ± 1.1 kcal/mol is observed for conductivity with respect to substrate temperature. Thus, oCVD process offers a straightforward means of controlling the conductivity of PEDOT to suit the various requirements of organic electronic devices, such as OLED,[42,43] OTFT,[44] and organic ROM-memory devices.[45] Therefore, its applications to the device can give opportunity of breakthrough for the organic electronics.

Acknowledgment. This research was supported by, or supported in part by, the U.S. Army through the Institute for Soldier Nanotechnologies, under Contract DAAD-19-02-D-0002 with the U.S. Army Research Office. The authors thank Mr. Sunyoung Lee for the measurement of UV−vis spectroscopy. The content does not necessarily reflect the position of the Government, and no official endorsement should be inferred.

References and Notes

(1) Groenendaal, B. L.; Jonas, F.; Freitag, D.; Pielartzik, H.; Reynolds, J. R. *Adv. Mater.* **2000**, *12*, 481−494.
(2) Kirchmeyer, S.; Reuter, K. *J. Mater. Chem.* **2005**, *15*, 2077−2088.
(3) Jonas, F.; Morrison, J. T. *Synth. Met.* **1997**, *85*, 1397−1398.
(4) Bredas, J. L.; Silbey, R. J. *Conjugated Polymers: The novel science and technology of highly conducting and nonlinear optically active materials*; Kluwer Academic Publishers: Dordrecht, 1991.
(5) Yamato, H.; Kai, K.; Ohwa, M.; Asakura, T.; Koshiba, T.; Wernet, W. *Synth. Met.* **1996**, *83*, 125−130.
(6) Groenendaal, L.; Zotti, G.; Aubert, P. H.; Waybright, S. M.; Reynolds, J. R. *Adv. Mater.* **2003**, *15*, 855−879.
(7) Kim, J.; Kim, E.; Won, Y.; Lee, H.; Suh, K. *Synth. Met.* **2003**, *139*, 485−489.
(8) Ha, Y. H.; Nikolov, N.; Pollack, S. K.; Mastrangelo, J.; Martin, B. D.; Shashidhar, R. *Adv. Funct. Mater.* **2004**, *14*, 615−622.
(9) Winther-Jensen, B.; Breiby, D. W.; West, K. *Synth. Met.* **2005**, *152*, 1−4.
(10) Jonas, F.; Heywang, G. *Electrochim. Acta* **1994**, *39*, 1345−1347.
(11) Jonas, F.; Krafft, W.; Muys, B. *Macromol. Symp.* **1995**, *100*, 169−173.
(12) Kobayashi, H.; Kanbe, S.; Seki, S.; Kigchi, H.; Kimura, M.; Yudasaka, I.; Miyashita, S.; Shimoda, T.; Towns, C. R.; Burroughes, J. H.; Friend, R. H. *Synth. Met.* **2000**, *111*, 125−128.
(13) Lock, J. P.; Im, S. G.; Gleason, K. K. *Macromolecules* **2006**, *39*, 5326−5329.
(14) Winther-Jensen, B.; West, K. *Macromolecules* **2004**, *37*, 4538−4543.
(15) Meng, H.; Perepichka, D. F.; Bendikov, M.; Wudl, F.; Pan, G. Z.; Yu, W. J.; Dong, W. J.; Brown, S. *J. Am. Chem. Soc.* **2003**, *125*, 15151−15162.
(16) Sotzing, G. A.; Briglin, S. M.; Grubbs, R. H.; Lewis, N. S. *Anal. Chem.* **2000**, *72*, 3181−3190.
(17) Ouyang, J.; Chu, C. W.; Chen, F. C.; Xu, Q. F.; Yang, Y. *J. Macromol. Sci., Pure Appl. Chem.* **2004**, *A41*, 1497−1511.
(18) Ouyang, J.; Xu, Q. F.; Chu, C. W.; Yang, Y.; Li, G.; Shinar, J. *Polymer* **2004**, *45*, 8443−8450.
(19) Kim, J. Y.; Jung, J. H.; Lee, D. E.; Joo, J. *Synth. Met.* **2002**, *126*, 311−316.
(20) Groenendaal, L.; Zotti, G.; Jonas, F. *Synth. Met.* **2001**, *118*, 105−109.
(21) Zhang, F.; Petr, A.; Peisert, H.; Knupfer, M.; Dunsch, L. *J. Phys. Chem. B* **2004**, *108*, 17301−17305.
(22) Johansson, T.; Pettersson, L. A. A.; Inganas, O. *Synth. Met.* **2002**, *129*, 269−274.
(23) Im, S. G.; Olivetti, E. A.; Gleason, K. K. *Appl. Phys. Lett.* **2007**, *90*, 152112.
(24) Sadki, S.; Schottland, P.; Brodie, N.; Sabouraud, G. *Chem. Soc. Rev.* **2000**, *29*, 283−293.
(25) Garreau, S.; Louarn, G.; Buisson, J. P.; Froyer, G.; Lefrant, S. *Macromolecules* **1999**, *32*, 6807−6812.
(26) Harima, Y.; Jiang, X. Q.; Kunugi, Y.; Yamashita, K.; Naka, A.; Lee, K. K.; Ishikawa, M. *J. Mater. Chem.* **2003**, *13*, 1298−1305.
(27) Meisel, K. D.; Vocks, H.; Bobbert, P. A. *Phys. Rev. B* **2005**, *71*.
(28) Chandrasekhar, P. *Conducting Polymers, Fundamentals and Applications: A Practical Approach*; Kluwer Academic: Dordrecht, 1999.
(29) Apperloo, J. J.; Groenendaal, L.; Verheyen, H.; Jayakannan, M.; Janssen, R. A. J.; Dkhissi, A.; Beljonne, D.; Lazzaroni, R.; Bredas, J. L. *Chem.—Eur. J.* **2002**, *8*, 2384−2396.
(30) Kiebooms, R.; Aleshin, A.; Hutchison, K.; Wudl, F. *J. Phys. Chem. B* **1997**, *101*, 11037−11039.
(31) Aleman, C.; Armelin, E.; Iribarren, J. I.; Liesa, F.; Laso, M.; Casanovas, J. *Synth. Met.* **2005**, *149*, 151−156.
(32) Skotheim, T. A.; Elsenbaumer, R. L.; Reynolds, J. R. *Handbook of Conducting Polymers*, 2nd ed.; M. Dekker: New York, 1998.
(33) Tran-Van, F.; Garreau, S.; Louarn, G.; Froyer, G.; Chevrot, C. *J. Mater. Chem.* **2001**, *11*, 1378−1382.
(34) Yamamoto, T.; Abla, M. *Synth. Met.* **1999**, *100*, 237−239.
(35) Chiu, W. W.; Travas-Sejdic, J.; Cooney, R. P.; Bowmaker, G. A. *Synth. Met.* **2005**, *155*, 80−88.
(36) Levenspiel, O. *Chemical Reaction Engineering*, 3rd ed.; Wiley: New York, 1999.
(37) Lee, K.; Cho, S.; Park, S. H.; Heeger, A. J.; Lee, C. W.; Lee, S. H. *Nature (London)* **2006**, *441*, 65−68.
(38) Prigodin, V. N.; Epstein, A. J. *Physica B: Condens. Matter* **2003**, *338*, 310−317.
(39) Li, Z. F.; Ruckenstein, E. *Macromolecules* **2002**, *35*, 9506−9512.
(40) Ruckenstein, E.; Li, Z. F. *Adv. Colloid Interface Sci.* **2005**, *113*, 43−63.
(41) Moore, W. J. *Physical Chemistry*, 4th ed.; McGraw-Hill: Boston, 1972.
(42) Koch, N.; Elschner, A.; Schwartz, J.; Kahn, A. *Appl. Phys. Lett.* **2003**, *82*, 2281−2283.
(43) Koch, N.; Kahn, A.; Ghijsen, J.; Pireaux, J. J.; Schwartz, J.; Johnson, R. L.; Elschner, A. *Appl. Phys. Lett.* **2003**, *82*, 70−72.
(44) Lee, K. S.; Blanchet, G. B.; Gao, F.; Loo, Y. L. *Appl. Phys. Lett.* **2005**, *86*.
(45) Moller, S.; Perlov, C.; Jackson, W.; Taussig, C.; Forrest, S. R. *Nature (London)* **2003**, *426*, 166−169.

MA0628477